Self-Structured Guanosine 5′-Monophosphate. A ^{13}C and ^{1}H Magnetic Resonance Study

Cherie L. Fisk,[1a] Edwin D. Becker,[1a] H. Todd Miles,*[1a,b] and T. J. Pinnavaia[1c]

Contribution from the National Institute of Arthritis, Diabetes, and Digestive and Kidney Diseases, National Institutes of Health, Bethesda, Maryland 20205, and the Department of Chemistry, Michigan State University, East Lansing, Michigan 48823. *Received June 11, 1981*

Abstract: The size and number of self-association complexes formed by $Na_2$5′-GMP in alkaline solution have been studied by proton and carbon-13 NMR spectroscopy. The temperature and concentration dependence of the two H8 structure lines appearing at 7.25 and 8.55 ppm is consistent with a 5′-GMP octamer formed by the head-to-tail stacking of two planar tetramer units. Carbon-13 spin–lattice relaxation times (T_1), line widths, and nuclear Overhauser enhancement (NOE) data for the corresponding C8 lines are in agreement with the size of an octamer, provided anisotropic rotation and hydrated dimensions are used in the calculations. A multiplicity of resonances is observed for all the carbons of structured $Na_2$5′-GMP, and the differences in relative area, T_1, line width, and NOE found among them are used to distinguish at least three self-associated species.

The guanosine moiety is unusual among nucleic acid bases in its ability to self-associate in aqueous solution into highly stable, regular structures. The self-structuring phenomenon is shown clearly in the formation of temperature-dependent anisotropic gels in acidic 3′- and 5′-guanosine monophosphate solutions[2–9] and the formation of stable regularly ordered complexes of the dianion in neutral and alkaline 5′-GMP (I) solutions.[10–13]

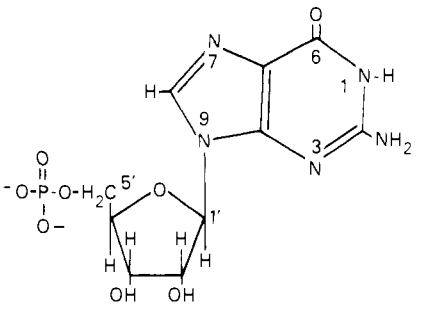

I

Temperature profiles of infrared absorbance for the 5′-GMP dianion show a cooperative transition (T_m = 9°, breadth ~ 13°, 0.1 M $Na_2$5′-GMP), indicating the formation of a regular ordered structure.[10] Analysis of the infrared and NMR spectra of the sodium salt of 5′-GMP in neutral solution, together with the spectra of certain alkyl- and amino-substituted derivatives, showed that II is almost certainly the basic building block of the self-associated form(s) of the dianion.[10,11] It is apparent that the 90° disposition of two hydrogen bond donors (N1–H, N2–H) and

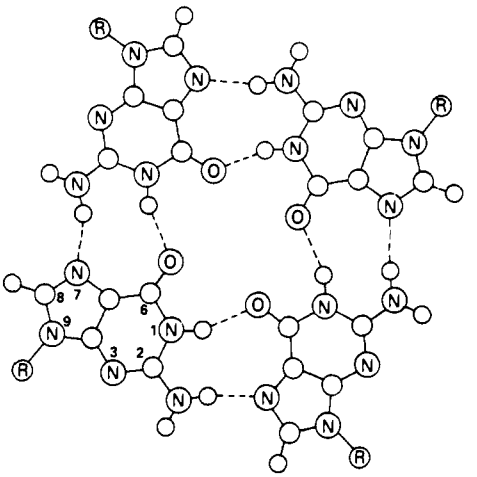

II

acceptors (C6=O, N7) in guanosine will favor association of the monomer into a planar tetrameric structure (II). With two hydrogen bonds per base (as compared with an average of 1.5 hydrogen bonds per base for the stable G-C pair), this structure is anticipated to be quite stable. X-ray diffraction studies of fiberlike bundles of 5′-GMP crystals from neutral solution provide evidence for further self-association of the tetramers into arrays of planar stacked plates.[12]

Several years ago we presented proton NMR data that further characterized the self-structuring process of the dianion, $Na_2$5′-GMP.[11] Under conditions of high concentration and/or low temperature, marked changes in the spectrum occur, with the emergence of new lines from species that must be exchanging only slowly. The changes are most clearly observed in the H8 region, as shown in Figure 1. The "outer" lines are separated by about 1.3 ppm—a relatively large association-induced proton chemical shift. The shift of associated 5′-GMP H8 lines is attributable to ring-current effects that could shift H8 lines upfield by as much as 0.9 ppm and electrostatic effects that could result in downfield shifts of as much as 0.5 ppm. Other proton NMR data[11] confirmed the participation of the amino protons in hydrogen bonds.

Further NMR studies disclosed the surprising result that the nature and extent of 5′-GMP association at neutral pH are highly specific for the alkali metal ions present in solution.[13] Na^+, K^+, and Rb^+ result in self-structure formation; Li^+ and Cs^+ do not do so to an appreciable extent.[13] In the case of the $Na_2$5′-GMP structure, the Na^+ could easily fit in the center of the planar tetramer (II) at a distance ~2.2–2.3 Å from the center of the carbonyl oxygens. This O–Na distance is very close to observed values, for example, in the Na^+ complex of an analogue of an-

(1) (a) National Institutes of Health; (b) request reprints from H. Todd Miles, Building 2, Room 201, National Institutes of Health, Bethesda, MD 20205; (c) Michigan State University.

(2) I. Bang, *Biochem. Z.*, **26**, 293 (1910).
(3) M. Gellert, M. N. Lipsett, and D. R. Davies, *Proc. Natl. Acad. Sci. U.S.A.*, **48**, 2013 (1962).
(4) H. T. Miles and J. Frazier, *Biochim. Biophys. Acta*, **79**, 216 (1964).
(5) F. B. Howard and H. T. Miles, *J. Biol. Chem.*, **240**, 801 (1965).
(6) P. K. Sarkar and J. T. Yang, *Biochem. Biophys. Res. Commun.*, **20**, 346 (1965).
(7) W. L. Peticolas, *J. Chem. Phys.*, **40**, 1463 (1964).
(8) J. F. Chantot, M. Th. Sarocchi, and W. Guschlbauer, *Biochimie*, **53**, 347 (1971).
(9) V. Sasisekharan, S. Zimmerman, and D. R. Davies, *J. Mol. Biol.*, **92**, 171 (1975).
(10) H. T. Miles and J. Frazier, *Biochem. Biophys. Res. Commun.*, **49**, 199 (1972).
(11) T. J. Pinnavaia, H. T. Miles, and E. D. Becker, *J. Am. Chem. Soc.*, **97**, 7198 (1975).
(12) S. Zimmerman, *J. Mol. Biol.*, **106**, 663 (1976).
(13) T. J. Pinnavaia, C. L. Marshall, C. M. Mettler, C. L. Fisk, H. T. Miles, and E. D. Becker, *J. Am. Chem. Soc.*, **100**, 3625 (1978).

0002-7863/82/1504-3307$01.25/0

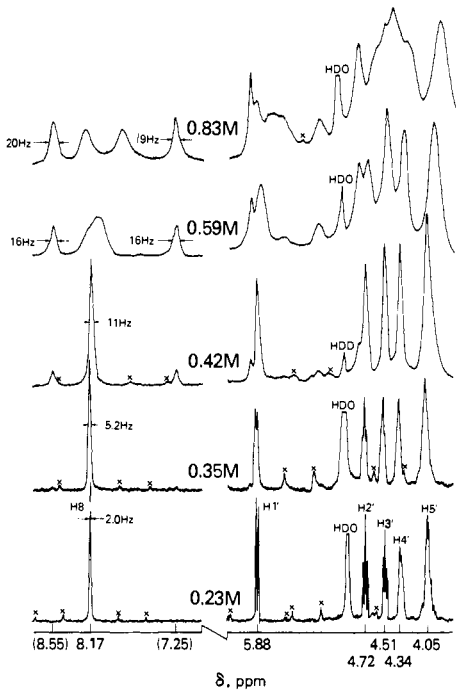

Figure 1. Proton NMR spectrum (220 MHz) of $Na_2$5′-GMP in D_2O solutions at 19 ± 1 °C. The chemical shifts are relative to TSP as internal standard and apply only to the 0.23 M solution. The values in parentheses are the concentration-independent shifts of the highest and lowest field H8 lines that appear in the remaining spectra. Line widths at half-maximum amplitude are provided for selected H8 resonances. The positions of spinning sidebands are marked "x" (reproduced from ref 11).

tamanide (average distance from Na^+ to carbonyl oxygen, 2.30 Å).[14] A fifth coordination to solvent above the tetramer plane is possible, by analogy to the pentacoordination observed in the antaminide analogue.[14] Coordination of Na^+ at the center of a tetramer would not necessarily inhibit stacking of two tetramer units to form an octamer. In the 5′-GMP case, a limiting of the stacked tetramers at the octamer stage would permit the stabilizing fifth coordination of each Na^+ to solvent H_2O.

To date, the self-structure of $Na_2$5′-GMP has been the most extensively studied and is the form on which we concentrate here. It affords the simplest proton NMR spectrum in the H8 region (Figure 1), the multiple lines indicating a chemical shift nonequivalence among tetrameric units, which could result from either a single species with an asymmetric overlap of stacked plates or several different species.

In previous communications we suggested the probable presence of rather small species for the $Na_2$5′-GMP self-associated complexes, such as octamers or dodecamers (two or three stacked plates). Recently Laszlo and co-workers[15] also examined possible structures and concluded hexadecamers and octamers are likely to be present. In this paper we extend the earlier 220-MHz ^1H NMR studies to give a quantitative measure of the size of at least one associated species, and we report on ^{13}C NMR spectra (68 MHz) of $Na_2$5′-GMP under conditions favoring self-structure formation. Several advantages are available with carbon-13 NMR spectroscopy. Typically, the carbon-13 resonances appear over a relatively large chemical shift range, which at 68 MHz covers some 12000 Hz. In addition, even at this field strength the relaxation of protonated carbons in diamagnetic liquids is dominated by single-bond C–H dipole–dipole interactions as modulated by molecular motion.[16] Therefore, measurement of the spin–lattice relaxation time, T_1,[17] the spin–spin relaxation time, T_2 (estimated from the line width), and the nuclear Overhauser enhancement (NOE)[18] permits, in a rigid molecule, direct estimates of rotational correlation times (τ_R) and molecular size.[19-24] Our analysis of plausible structures for the associated species is complemented by a molecular modeling approach in the work of Pinnavaia et al.[25]

Experimental Section

Sample Preparation. Only the sodium salt, $Na_2$5′-GMP, was used in this work (abbreviated 5′-GMP). 5′-GMP was purchased from PL Biochemicals (Milwaukee, WI). 5′-GMP concentrations were measured by using the absorbance at 252 nm (ϵ 1.34 × 10^4). Viscosities were determined with a No. 75 Cannon-Ubbelohde semimicro type viscometer (Cannon Instrument Co., State College, PA) in a water bath controlled at 5 °C. Samples for ^{13}C T_1 measurements were passed through a Chelex-100 column (Bio-Rad Laboratories, Rockville Center, NY) to remove paramagnetic impurities and were lyophilized at least once from D_2O (Merck Isotopes, St. Louis, MO) prior to dissolving in 99.8% D_2O. Sample volumes of 1–1.2 mL (deoxygenated with a 10-min nitrogen gas purge for ^{13}C T_1 measurements) were used in flat-bottom 10-mm NMR tubes (Wilmad Glass, Buena, NJ) with a 10-mm Wilmad microcell to prevent vortexing. The small volume contained the sample within the decoupling coil, thus reducing gradients under decoupling conditions. Samples used for proton NMR measurements were repeatedly lyophylized from D_2O to remove exchangeable protons. The ^{13}C and ^1H samples also contained 1 mM Na_2EDTA.

Proton NMR. Spectra at 220 MHz were obtained on a Varian HR-220 spectrometer operating in the Fourier transform mode. Spectra at 360 MHz were obtained on a Bruker HFX-10 spectrometer at the Stanford Magnetic Resonance Laboratory, Stanford, CA. Sample temperature was determined by calibration of the probe with ethylene glycol and methanol. Spin–lattice relaxation times were measured by the inversion–recovery method.[17]

Carbon-13 NMR. Spectra were obtained at 67.8 MHz on a spectrometer consisting of a Bruker high-resolution superconducting magnet, a Bruker 10-mm probe, and radio-frequency electronics built by the Biomedical Engineering and Instrumentation Branch, NIH. During the course of the study, the spectrometer was coupled in turn to Nicolet 1080 and 1180 computers. The high salt concentrations used in these studies resulted in considerable dielectric heating under normal proton-decoupling conditions. This could be compensated for, in part, by a relatively large chilled nitrogen gas flow through the probe. Operation at 5 °C necessitated a two-level gated-decoupling technique whereby about 0.7 W of decoupling power remained on at all times other than during the acquisition time (AT) when power was increased to 4–4.5 W. Spin–lattice relaxation times were measured by the fast inversion recovery $(180°-\tau-90°-AT-t_d)_n$ pulse sequence.[26]

The nuclear Overhauser enhancement (NOE) of the carbon-13 signals is reported as an intensity ratio $(1 + \eta)$.[18] NOE values were measured in two successive single 90° pulse experiments $(90°-AT-t_d)_n$ where ~0.7 W of power was gated either on (NOE) or off (no NOE) during the delay, t_d, and ~4 W was always on during time AT. Data collection was generally delayed at least 128 pulse sequences in order to ensure temperature equilibration under the gated-decoupling conditions.

The sample temperatures for ^{13}C experiments were measured by the following procedure:[27] the spinning sample was equilibrated in the probe

(14) I. L. Karle, *Biochemistry*, **13**, 2155 (1974).
(15) M. Borzo, C. Detellier, P. Laszlo, and A. Paris, *J. Am. Chem. Soc.*, **102**, 1124 (1980); C. Detellier and P. Laszlo, *J. Am. Chem. Soc.*, **102**, 1135 (1980), and references cited in these papers.
(16) R. S. Norton, A. O. Clouse, R. Addleman, and A. Allerhand, *J. Am. Chem. Soc.*, **99**, 79 (1977).
(17) R. L. Vold, J. S. Waugh, M. P. Klein, and D. E. Phelps, *J. Chem. Phys.*, **48**, 3831 (1968).
(18) K. Kuhlman, D. M. Grant, and R. K. Harris, *J. Chem. Phys.*, **52**, 3439 (1970).
(19) A. Abragam, "The Principles of Nuclear Magnetism", Oxford University Press, London (1961).
(20) I. Solomon, *Phys. Rev.*, **99**, 559 (1955).
(21) A. Allerhand, D. Doddrell, and R. Komoroski, *J. Chem. Phys.*, **55**, 189 (1971).
(22) D. Doddrell, V. Glushko, and A. Allerhand, *J. Chem. Phys.*, **56**, 3683 (1972).
(23) N. Bloembergen, E. M. Purcell, and R. V. Pound, *Phys. Rev.*, **73**, 679 (1948).
(24) D. E. Woessner, *J. Chem. Phys.*, **37**, 647 (1962).
(25) T. J. Pinnavaia, C. L. Marshall, and E. L. Brown, manuscript in preparation.
(26) D. Canet, G. C. Levy, and I. R. Peat, *J. Magn. Reson.*, **18**, 199 (1975).
(27) Alternate methods of measuring sample temperature were not used for the following reasons: Using a thermocouple immersed in the sample while it equilibrated in the probe was found to reduce the amount of dielectric heating from the decoupler and thus to change the sample temperature. Shielding the thermocouple cable from RF interference appeared to increase this effect even further.

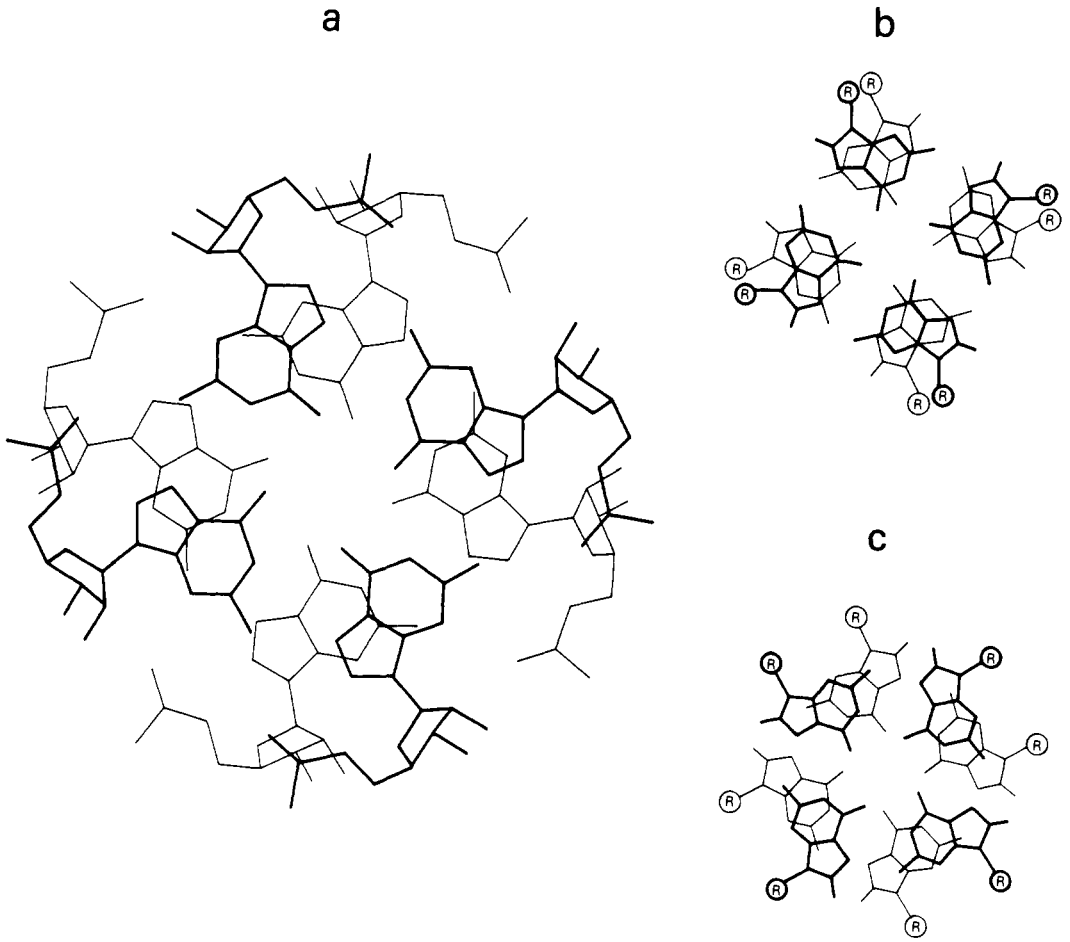

Figure 2. The relative disposition of 5'-GMP base units in various octamer structures formed by the stacking of planar tetramers (a) hard-to-tail (HT), +30° twist; (b) tail-to-tail (TT), +30° twist; (c) tail-to-tail (TT), −30° twist. Bold-faced structures lie in an upper plane.

under appropriate decoupling conditions, then the sample was removed from the probe and a glass-enclosed copper–constantan thermocouple (connected to a Doric Trendicator-400 digital meter) inserted. The procedure could be accomplished within 20 s, the major source of error arising from vertical and horizontal gradients in the tube of about ±1.5 °C for 0.7 M 5'-GMP.

Data Analysis. T_1 values were calculated from a fit of experimental points to the generalized relation[28]

$$M(\tau) = M(\infty)(1 - [1 + A(1 - e^{-W/T_1})]e^{-\tau/T_1}) \quad (1)$$

where $M(\tau)$ is the peak amplitude corresponding to the recovery time τ; A is an instrumental parameter correcting for imperfections in pulse width, H_1 field inhomogeneity, or off-resonance effects (equals 1 in the ideal inversion–recovery case); and W is set to the pulse delay t_d. In the case of ^{13}C measurements, a sample of neat ethylene glycol of matching dimensions was used to measure A with the sample pulse widths and frequency offset (1 kHz) as for experiments measuring the C8 5'-GMP resonance lines. This value (typically 0.8) resulted in a good fit of 5'-GMP data. In the case of ^1H measurements, $T_1 \ll W$, and the term $\exp(-W/T_1)$ was thus dropped from eq 1. In several experiments, sufficient proton data were available such that parameter A could also be determined. This value was then used in some cases in order to fit with the logarithmic form of eq 1. The data were fit by using least-squares regression packages on the NIH Nicolet 1180[29] or DEC-10 (MLAB program)[30] computers.

Deconvolution of overlapping carbon-13 lines was accomplished on the 1180 computer with the Nicolet "CAP" program.[29]

Computer Modeling. Molecular modeling of stacked GMP species was accomplished on the NIH DEC-10 computer with the XRAY molecular display program developed by Feldmann.[31] Coordinates for four-stranded poly(guanylic acid)[32] served as the basis for generating a head-to-tail stacked octamer with a twist of 30°. The PO–C3' bonds were first disconnected, and an additional OH was added to the ribose 3'-carbon. Changes in twist angle and inversion of one tetramer relative to the other (to generate head-to-head or tail-to-tail octamers) then resulted in the structures of Figure 2.

Ring-current shifts of atoms in the stacked 5'-GMP configurations were calculated either by a DEC-10 version of a program kindly supplied to us by D. B. Arter and P. G. Schmidt[33] (on the basis of equations from Giessner-Prettre and Pullman, 1970)[34] or by superposition of ring-current isoshielding contours from Giessner-Prettre and Pullman (1976)[35] on the structures of Figure 2.

Calculations of rotational diffusion and NMR relaxation parameters for GMP were performed on the NIH DEC-10 computer using MLAB[30] and RELAXG[36] programs, respectively.

Results and Discussion

Both infrared and proton NMR data show clearly the cooperative nature of the transition of 5'-GMP to associated forms. Such transitions are commonly found in polymeric systems; in 5'-GMP at pH 5 a long helical structure is formed, leading to gel formation. In neutral solution, however, there is no gel formation, and it is reasonable to assume that the larger negative charge (two per nucleotide rather than one in acid solution) will provide sufficient electrostatic repulsion to terminate association short of an "infinite" chain. The size and number of shorter species are a major concern of the work reported here.

(28) E. D. Becker, J. A. Ferretti, R. K. Gupta, and G. H. Weiss, *J. Magn. Reson.* **37**, 381 (1980).
(29) "NTCFT-1180 Users Manual", Nicolet Technology Corp., Mountain View, CA.
(30) G. D. Knott, *Comput. Programs Biomed.*, **10**, 271 (1979).
(31) R. J. Feldmann, *Annu. Rev. Biophys. Bioeng.*, **5**, 477 (1976).
(32) S. B. Zimmerman, G. H. Cohen, and D. R. Davies, *J. Mol. Biol.*, **92**, 181 (1975).
(33) D. E. Arter and P. G. Schmidt, *Nucleic Acids Res.*, **3**, 1437 (1976).
(34) C. Giessner-Prettre and B. Pullman, *J. Theor. Biol.*, **27**, 87 (1970); C. Giessner-Prettre, B. Pullman, P. Borer, L-S Kan, and P. O. P. T'so, *Biopolymers*, **15**, 2277 (1976).
(35) C. Giessner-Prettre and B. Pullman, *Biochem. Biophys. Res. Commun.*, **70**, 578 (1976).
(36) D. A. Torchia, J. R. Lyerla, Jr., and A. J. Quattrone, *Biochemistry*, **14**, 887 (1975).

Table I. Proton T_1 Values for $Na_2$5′-GMP H8 Lines[a]

MHz	concn, M	t, °C	T_1, s H_α	H_β	H_γ	H_ϵ	H_δ
220	0.41	0	2.49	1.33	1.24	0.98	2.33
220	0.59	1	2.17[b]	1.59[b]	1.54[b]		2.08[b]
220	0.59	19	1.96[c]	0.75[c]	0.81[c]		1.92[c]
220	0.85	8	2.62	1.51	1.46		2.45
360	0.85	5	4.14	2.94	2.84		3.90
360	0.85	18	3.83	1.89	1.79		3.43
360	0.85	36	1.80	1.46			1.72

[a] Proton numbering follows Figure 4. [b] T_2* values (from line width measurements) for H_α, H_β, H_γ, and H_δ are 1.6, 1.4, 1.4, and 1.5×10^{-2} s, respectively. [c] T_2* values (from line width measurements) for H_α, H_β, H_γ, and H_δ are 2.6, 1.3, 1.2, and 2.6×10^{-2} s, respectively.

Size of the Associated Species. Because of the slow exchange displayed in the proton NMR spectrum (Figure 1), lines due to associated and unassociated species can be distinguished. Thus measurements of equilibria can be made directly rather than by invoking one of several possible models needed in the presence of rapid exchange. The peaks most clearly resolved in Figure 1 are the "outer" peaks in the H8 region at 8.55 and 7.25 ppm. The intensities of these outer lines are equal, within experimental error, under all conditions of temperature (see Figure 2, ref 11) and concentration (Figure 1) that we have investigated. In addition, the proton T_1 and T_2 data obtained for these outer lines parallel each other under varied experimental conditions (Table I), and the behavior of the two lines in the presence of paramagnetic ions is similar.[11] We conclude that they unquestionably belong to the same species.

The presence of two lines of equal intensity for H8 separated by 1.30 ppm leads us (as detailed below) to the conclusion that this species is an octamer in which one tetrameric plane is stacked above the other, with the sense of hydrogen bonds the same, and one tetramer is twisted relative to the other about the 4-fold axis. We refer to this species as a head-to-tail (HT)[37] octamer.

Evidence for stacking of GMP tetramers in a HT array similar to poly(G)[32] has been provided by X-ray diffraction studies of acid 3′-GMP[3] and by Zimmerman's study of small fiberlike bundles of 5′-GMP crystals from neutral solution.[12] These results indicate that the stacking of tetramers is helical, with a twist near 30°. Model building studies demonstrated that in such a structure certain favorable interplanar hydrogen-bonding patterns may exist, for example, with the 5′-phosphates of one tetramer hydrogen bonding to the 3′-hydroxyls of the other unit.[12] Pinnavaia et al.[25] assess these possibilities in a systematic fashion.

This type of HT octamer (probably with a twist of 30° in analogy with the X-ray work) can account for the outer lines of the H8 spectrum of 5′-GMP. This structure is depicted in Figure 2a. In this case the chemical shift of H8 in the four equivalent molecules making up the upper tetramer (HT + 30° u in Table II) is affected by ring currents from the purine rings of the lower tetramer, while H8 in the lower tetramer (HT + 30° l) in Table II) falls outside the higher isoshielding contours of the upper rings but might well be influenced by the negative charges on the nearby phosphate groups.

Alternative structures can easily be shown to be incompatible with the proton NMR data. Consider, first, a larger number of tetramer planes stacked in a HT arrangement to give a dodecamer, hexadecamer, or higher species. Analysis of ring-current effects (see Figure 2a) shows that each H8 in tetramer planes above the lowest would be nearly equally affected, whereas H8's in the bottom plane are little influenced. As a result, a HT species consisting of n tetrameric planes would be expected to give rise to an H8 spectrum with a low-field line (ca. 8.55 ppm) and $n - 1$ lines of equal intensity closely spaced at higher field (ca. 7.25 ppm). The observed equality in the areas of the two lines observed for H8 rules out all HT species except the octamer.

Other possible structures can also be ruled out as the species responsible for the "outer" lines. Head-to-head (HH) and tail-to-tail (TT) octamers can be considered. Figure 2 shows examples of these stacking patterns. HH and TT structures would be formed by inverting one of the tetrameric planes, so that the sense of the hydrogen-bond arrangements is clockwise in one tetramer and counterclockwise in the other. These structures are related to the inverted base pairs discussed by Gupta and Sasisekharan.[38] Both HH and TT structures give rise to symmetrically equivalent H8 protons in all eight positions, hence to only a single H8 line. Thus, these symmetrical structures (and higher polymers of similar structure) can be ruled out as candidates since the outer lines have such disparate chemical shifts. (These species may well be re-

Table II. Calculated Ring-Current Shifts for Head-to-Tail (HT) Models of 5′-GMP Octamers

unit[b]	ring-current shift[a] C1′	C8	C5	C6	C2	C4	H8
I. Giessner-Prettre and Pullman, 1970[34]							
HT + 30° u HT − 30° l	0.02	−0.27	−0.32	−0.18	−0.18	−0.12	−0.17
HT + 30° l HT − 30° u	−0.01	−0.01	−0.15	−0.15	−0.68	−0.28	0.02
tetramer (in plane)	0.05	0.09	0.14	0.21	0.18	0.10	0.08
II. Giessner-Prettre and Pullman, 1976[35]							
HT + 30° u HT − 30° l	−0.12	−0.52	−0.59	−0.52	−0.48	−0.37	−0.37
HT + 30° l HT − 30° u	−0.12	−0.25	−0.46	−0.46	−1.00	−0.51	−0.17

[a] The shift is expressed in ppm; a negative shift corresponds to an upfield shift. [b] The HT structure corresponds to that of Figure 2a. An upper unit of a 5′-GMP octamer is designated by u, a lower unit by l. Values of +30° or −30° refer to HT structures with a helical twist of +30° and −30°, respectively.

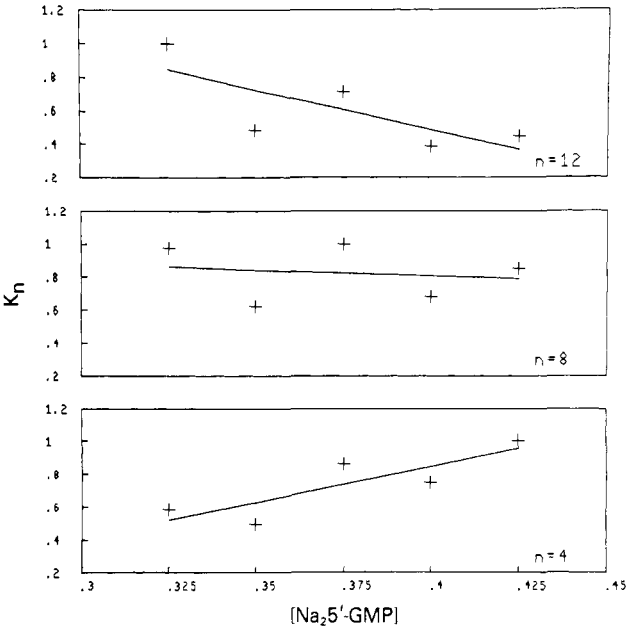

Figure 3. Plot of normalized association constant, K_n, vs. concentration of $Na_2$5′-GMP (buffered to pD 8 with Na_2HPO_4). Values for K were calculated from the equation $K = [n\text{-mer}]/[\text{monomer}]^n$ for three values of n (4, 8, and 12). The n-mer and monomer concentrations were obtained from the relative areas of the H8 lines at 7.25 ppm ($[n\text{-mer}]/2$) and 8.17 ppm ([monomer]). The values of K within a given $n = 4$, $n = 8$, and $n = 12$ calculation have been normalized to give K_n before plotting. The solid lines represent least-squares fits of the data.

(37) The "Head" and "tail" of 5′-GMP are arbitrarily defined here as follows: the side of the base facing up from the page when 5′-GMP is drawn with the five-membered ring to the right is called the head; that facing down is called the tail.

(38) G. Gupta and V. Sasisekharan, *Nucleic Acids Res.*, **5**, 1639 (1978).

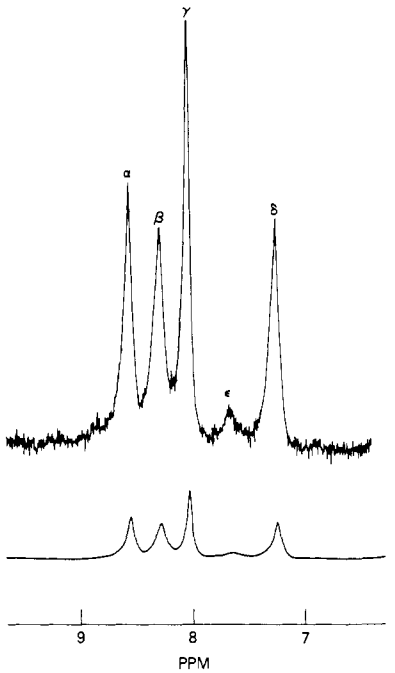

Figure 4. Proton NMR spectrum (220 Mhz) of the H8 region of 0.46 M $Na_2$5'-GMP at 0 °C.

sponsible for other lines observed in the H8 spectrum.)

We have also made an independent assessment of the assignment of the outer lines to an octamer by measuring the areas under these in relation to that under the "monomer" peak at 8.0 ppm as a function of concentration at 19 °C. Because of the high-order concentration dependence, measurements were made over only a relatively narrow range of concentration—0.32–0.42 M. Nevertheless, it is possible to obtain sufficient data to distinguish various possible species. Figure 3 provides a plot of the equilibrium expressions $(C_n)/(C_m)^n$, where m and n refer to monomer and n-mer, respectively. Since the planar tetrameric arrangement II is well established, we need only consider n as multiplies of 4. In spite of some scatter, Figure 3 shows clearly that $n = 8$ provides an essentially constant value of the equilibrium expression, while $n = 4$ and $n = 12$ do not. (Note that the slopes for $n = 4$ and $n = 12$ are opposite in sign.) This measurement is less definitive than our previous arguments in favor of the HT octamer, since in principle the "monomer" peak might also contain contributions from higher species, such as tetramers. The fact that $n = 8$ gives a rather good fit suggests that the peak at 8.17 ppm is principally monomer.

Proton Chemical Shifts and Relaxation Measurements. Proton NMR spectra previously obtained for the H8 region of self-structured $Na_2$5'-GMP indicated a multiplicity of species due to the appearance (Figure 1) of four distinct H8 lines differing in both stability and NMR relaxation parameters.[11] We have now performed additional experiments, which indicate that at least five (rather than four) H8 lines are found under conditions favoring self-structure formation (Figure 4). The 5'-GMP samples for these spectra were carefully prepared in order to eliminate any possibility that the line appearing near 7.6 ppm is actually an NH resonance (from exchange with residual HOD). Analysis of the solvent shows the concentration of HOD to be less than 0.4%, an amount inadequate to produce the observed signal. Moreover, the absence of the much stronger NH line at ~9.2 ppm confirms that the fifth peak at 7.66 ppm is not an NH peak.

The fifth line (H_ϵ, Figure 4) has a T_1 value of 0.98 s (19°, 0.41 M), which is in the same range as lines H_β and H_γ. This T_1 value, however, is half that of the two outer lines, H_α and H_γ (Table I). These differences in T_1 values are a major reason for ascribing the outer lines (H_α, H_δ) to an associated species different from that of the inner lines (H_β, H_γ, H_ϵ). The proton relaxation data for the H8 self-structure lines summarized in Table I indicate that $T_1 > T_2$, and thus the rotational correlation rate of the GMP

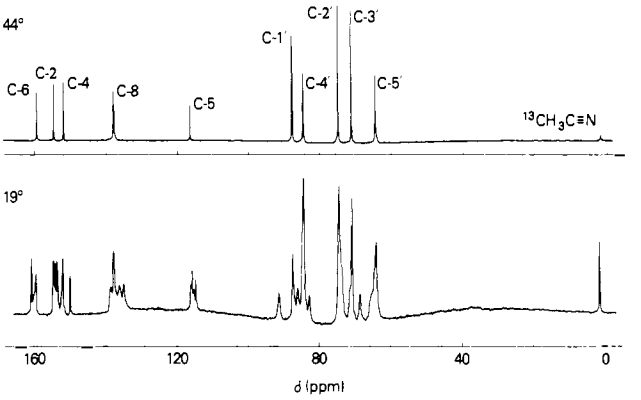

Figure 5. Proton-decoupled ^{13}C FTNMR spectrum of 0.71 M $Na_2$5'-GMP in D_2O at 44 °C and 19 °C.

complexes is slow on the NMR time scale ($2\pi\nu^{-1} < \tau_R$). Also, the T_1 values are frequency dependent, further indicating the slow-tumbling nature of the complexes.

Carbon-13 Chemical Shifts. ^{13}C NMR spectra of a concentrated solution of 5'-GMP (0.71 M in D_2O, pD 8.8) at two temperatures are shown in Figure 5 and 6. The resonances of the monomer observed at 44 °C (Table III) are assigned by reference to literature values.[39]

In direct analogy to the ^{1}H NMR data,[11] decreasing the probe temperature results in (i) a broadening and frequency shift of the 5'-GMP monomer carbon-13 lines and (ii) the appearance of additional "structure" lines which can be ascribed to the self-assembled complex. Figure 6 shows a ^{13}C NMR spectrum of 0.7 M 5'-GMP at 17 °C obtained under instrumental conditions where signal intensity of protonated carbons is related to concentration (long pulse delay, gated decoupling to suppress any NOE). An insert to Figure 6 gives the ^{1}H NMR spectrum of the H8 region for the sample at 19 °C.

We have simulated the spectrum in Figure 6 under the assumption that each carbon contributes four structure lines. Results of this curve fitting are shown below each spectral region, with chemical shifts and line widths reported in Table III. The match between observed and simulated spectra is good.

Assignment of each of the structure lines found in the simulated spectrum to a specific 5'-GMP carbon is unambiguous except for carbon pairs 2 and 4, 1' and 4', and 2' and 3'. The C1' and C4' lines can be distinguished by single-frequency proton decoupling as assigned. For C2 and C4 (nonprotonated) and C2' and C3' (close to proton frequency), the structure lines are tentatively assigned to the carbon nearest in monomer chemical shift.

A large range of chemical shift values is observed for structure lines attributable to a single 5'-GMP carbon (labeled a–d, Figure 6, Table III). Base carbons 6, 2, 4, 8, and 5 have structure lines covering ranges 1.1, 1.2, 2.1, 3.6, and 1.4 ppm, respectively. Likewise in the ribose region, ranges of 7.0, 3.2, 1.1, 2.7, and 1.6 ppm are found for structure lines attributable to carbons 1', 4', 2', 3', and 5', respectively. Of equal significance is the extent to which these structure lines are shifted to low or high field relative to the corresponding unstructured resonances. For example, aromatic lines C8a–d of the self-structure at 19° are shifted +0.64, −0.21, −1.79, and −3.01 ppm from their positions at 44°. In the ribose region, shifts of +3.9, −0.16, and −3.1 ppm are observed for the C1'a–d resonances. Other shifts of similar magnitude are present throughout the spectrum.

Observation of both large low-field (positive) and high-field (negative) chemical shifts in the structure lines attributed to a single carbon at 5'-GMP reflects the complexity of the shielding in this system. The chemical shift values of the 5'-GMP residue associated in stacked hydrogen-bonded planar tetramers are an-

(39) D. E. Dorman and J. D. Roberts, *Proc. Natl. Acad. Sci. U.S.A.*, **65**, 19 (1970); H. H. Mantsch and I. C. P. Smith, *Biochem. Biophys. Res. Commun.*, **46**, 808 (1972); M. Blumenstein and M. A. Raftery, *Biochemistry*, **12**, 3585 (1973).

Table III. Carbon-13 NMR Parameters of $Na_2$5′-GMP[a]

carbon	chem shift,[b] 44 °C	structure line	chem shift[b] 19 °C	chem shift[b] 19 − 44 °C	LW,[c] Hz	rel area[c]	species[d]
C6		a, b	158.9	+1.26	9	0.34	I,I
		c	158.3	+0.7	37	0.28	II
	157.65	d	157.81	+0.17	15	0.31	III
C2	152.88	a	152.80	−0.08	16	0.36	III
		b	152.34	−0.54	9	0.19	I
		c	152.2[e]	−0.68	37	0.20	II
		d	151.82[f]	−1.06	9	0.10	I
C4		a	151.60	+0.42	9	0.19	I
		b	150.5	+0.3	37	0.29	II
	150.18	c	150.17	−0.01	16	0.39	III
		d	148.14	−2.04	9	0.19	I
C8		a	136.95	+0.64	37	0.20	I
	136.31	b	136.1	−0.21	31	0.36	III
		c	134.52	−1.79	54	0.24	II
		d	133.30	−3.01	40	0.20	I
C5	114.88	a	114.67	−0.21	16	0.30	III
		b	114.29	−0.59	9	0.20	I
		c	113.82	−1.06	37	0.32	II
		d	113.3	−1.58	6	0.17	I
C1′		a	90.13[g]	+3.90	31	0.20	I
	86.23	b	86.07[g]	−0.16	27	0.33	III
		c, d	83.1[e,g]	−3.1	31, 49	0.20, 0.24	I,II
C4′		a	84.76[g]	+1.66	31	0.20	I
	83.10	b, c	83.07[e,g]	−0.03	27, 49	0.35, 0.24	III,II
		d	81.55[g]	−1.55	31	0.20	I
C2′		a	73.40[e]	+0.1	31	0.20	I
	73.29	b	73.08[e]	−0.21	27	0.38	III
		c	72.6[e]	−0.69	31	0.20	I
		d	72.3[e]	−1.0	49	0.20	II
C3′		a	72.3[e]	+2.7	31	0.20	I
		b	70.0	+0.51	49	0.24	II
	69.49	c	69.45	−0.04	27	0.35	III
		d	67.33	−2.16	31	0.20	I
C5′		a	64.4	+1.6	31	0.24	II
		b	63.8	+1.0	31	0.20	I
		c	63.1	+0.4	31	0.20	I
	62.75	d	62.73	+0.02	27	0.35	III

[a] 0.71 M in D_2O, pD 8.8. [b] Measured in ppm at 68 MHz relative to internal 13-CH_3CN. [c] LW (line width before filtering) and relative area are measured from the computer curve fits of Figure 6. Areas have been normalized to 1 for each carbon atom. [d] The rationale for assignment to a particular species is discussed in the text. [e] Position determined by curve fitting. [f] Assignment ambiguous; assigned to carbon nearest in chemical shift in monomer. [g] Assigned by double resonance experiment.

ticipated to differ significantly from these of the unassociated monomer observed at higher temperature. Of the potential sources of these chemical-shift perturbations, the following are considered to be most important: (i) the magnetic anisotropy (ring currents) of neighboring bases, (ii) hydrogen-bond formation and Na^+ coordination, (iii) electric-field effects due to proximity to the dianionic phosphate or Na^+, and (iv) generalized solvent effects that may result from the removal of the 5′-GMP base from a primarily aqueous to a more hydrophobic environment.

Quantitative evaluation of these effects is difficult because of the multiplicity of structures and lack of precision in estimating each shielding parameter. In particular, the highly anisotropic geometries of these proposed stacked tetramer complexes suggest that base nuclei on different layers will experience significantly different ring-current shifts as a function of the interplanar distance, the twist angle, and the stacking sense. Estimates of the ring-current shielding in purine and pyrimidine moieties have been reported by Geissner-Prettre and Pullman for calculations where local atomic anisotropies were either disregarded[34] or taken into account.[35] We have found that, even in the case where local atomic anisotropies are included and thus the shielding values substantially increased (Table II), such calculations generally underestimate the observed range of structure line shifts (Table III). At least one spectral feature can, however, be qualitatively explained in terms of our model structures. In particular, the carbonyl of 5′-GMP (C6) participates in both hydrogen bonding to the N1-H and electrostatic ion–dipole interaction with the central Na^+. Both hydrogen bonding and binding to Na^+ would deshield a participating carbonyl. In addition, our calculations also indicate that C6 will generally be the atom most affected by ring-current deshielding effects in the plane of the tetramer (Table II). Therefore, all of these may well contribute to counteract possible ring-current shieldings in the stacked units and thus result in low-field shifts in all C6 structure lines.

Additional information about the nature of the associated species is available in the obvious differences in line width among resonances attributable to a specific 5′-GMP carbon. This is particularly noticeable in nonprotonated carbons where several relatively sharp lines (for example, C2b,d and C5b,d) stand out among other broader structure lines. When correlated with T_1 and NOE results for protonated carbons presented in the following section, this evidence suggests the presence of at least three species (indicated in Table III by I, II, and III). In order to focus on these differences, we have chosen to study the relaxation behavior of protonated carbons of 5′-GMP. The C8a–d and C1′ a lines have been studied in detail as presented in the following section.

Carbon-13 Relaxation Measurements. The spin–lattice relaxation of the ^{13}C resonances of 0.7 M 5′-GMP at 5 °C is illustrated in Figure 7. This fast inversion–recovery (FIR) experiment was designed to measure T_1 data for protonated carbons in the system, the delay being too short for meaningful discrimination between nonprotonated carbon T_1 values. It is apparent from this figure that at least three different T_1 values characterize the relaxation behavior of resolved C–H carbons in this system. Relaxing most rapidly are the lines labeled C8b, C1′b, C4′bc, C2′bc, C3′c, and C5′d. These are all lines we assign to one 5′-GMP species, designated III in Table III. On the other hand, lines C8a and d, C1′a, C4′a and d, and C3′d have slower but similar recovery curves. These correspond to another species, I, as identified in Table III. Other lines are either unresolved or have intermediate

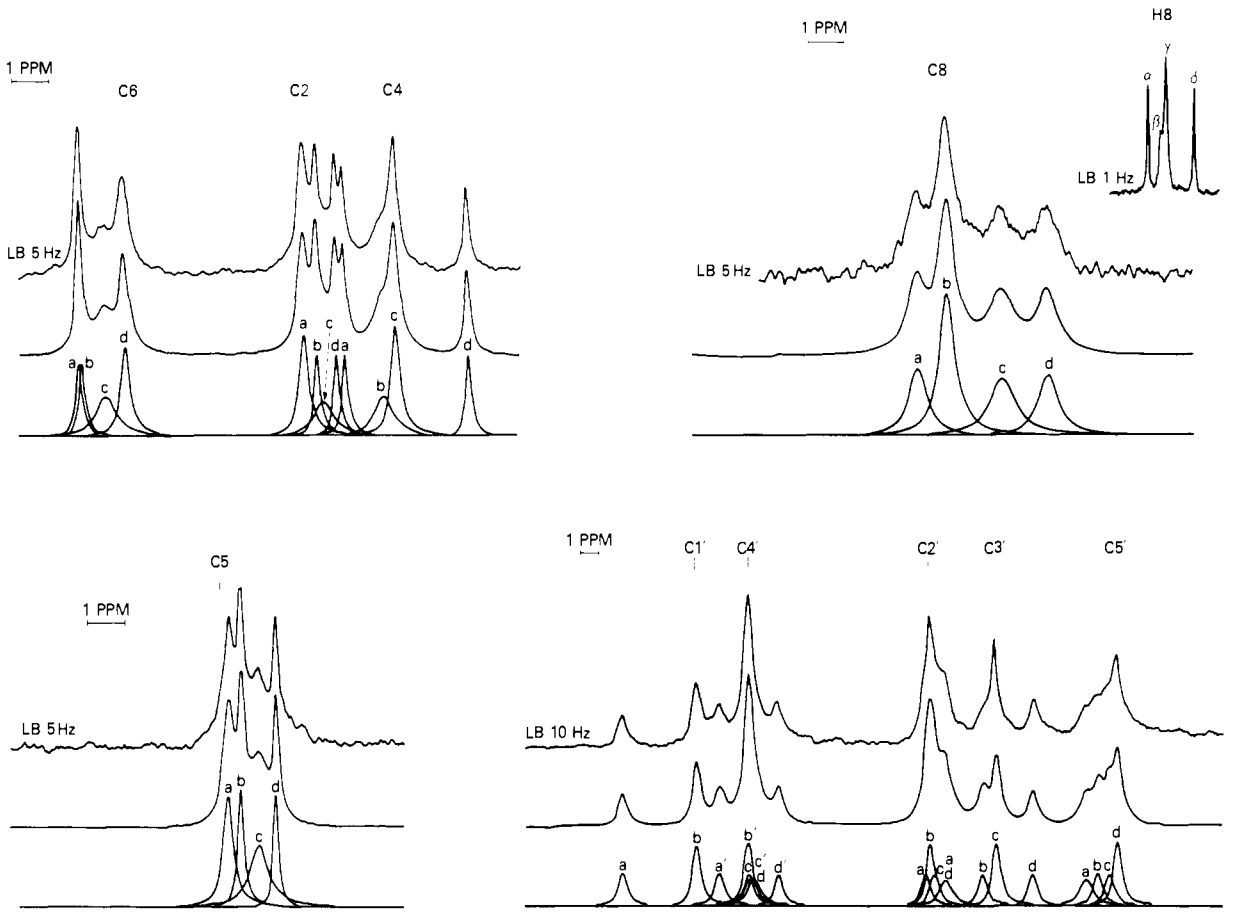

Figure 6. Expanded plots of the proton-decoupled ^{13}C FTNMR spectrum of 0.70 M $Na_2$5′-GMP in D_2O at 17 °C where the NOE has been suppressed by gated decoupling (90° pulse, 3.8K acquisitions, 16-s repetition time). Upper trace for each region shows experimental curve, lower two traces the result of curve fitting on the Nicolet computer (see Table III for parameters of individual lines). Also shown is the 220 MHz ^1H NMR spectrum of the H8 region of the same sample at 19 °C.

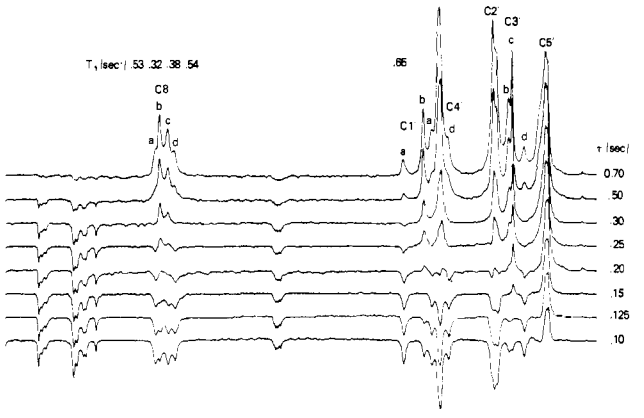

Figure 7. Fast inversion–recovery sequence, $(180°-\tau-90°-AT-t_d)n$, for 0.66 M $Na_2$5′-GMP in D_2O at 5 °C. A 40-μs 180° pulse (τ), 1.5 s delay (t_d), 16K acquisitions (n), 0.06-s acquisition time (AT), 2K data points, 2K zero filling, and 10-Hz line broadening were used. The pulse was positioned 1 kHz upfield from the C8 lines (QPD detection).

T_1 values such as line C8c (species II). The results of an NOE experiment also distinguish among lines: C8b,c and C1′b show a small but measurable NOE (1.3–1.5), while other C8 and C1′ structure lines are at the NOE minimum (1.2).[40] The qualitative value of these data lies in determination of the number of structured 5′-GMP species present in solution. We will focus on the (protonated) base C8 nuclei, which, as part of a rigid, hydrogen-bonded, Na^+-bonded, planar array, are anticipated to have a simple pattern of motion where internal rotation would not contribute. The most probable explanation for the different T_1, T_2, and NOE values among the C8 structure lines is that at least three species of significantly different molecular geometry are present (since there are three time classes).

The Number of Self-Associated Species. The proton and carbon-13 data point to at least three forms of self-associated 5′-GMP, species I, II, and III, which have the following characteristic spectral features: I is the narrowest line for nonprotonated carbons, has the longest T_1 values measured for protonated carbons, has no NOE (1.0–1.2) as measured for protonated carbons, and corresponds to two resonances for each carbon atom. This is the same species giving rise to the outer H8 lines (H_α, H_δ) in the proton NMR spectrum, which we assign to the head-to-tail octamer, HT. II is the broadest ^{13}C line for each carbon and has an intermediate T_1 measured for protonated carbons. This species is found in the proton H8 region as H_β. III shifts into the "monomer" line at high temperatures or low concentrations and has a small but measurable NOE and the shortest T_1 values. This species is found in the proton H8 region as H_γ.

Presumably yet another species, IV, visible only in proton spectra (H_ϵ, Figure 4), also exists in structured 5′-GMP solutions.

In the following section, we focus on an estimation of the size of species I from the ^{13}C spin–lattice relaxation time.

A Model of Motion for Stacked 5′-GMP. 5′-GMP monomers associating into planar tetramers and higher-order stacked tetramers result in structures most closely resembling axially symmetric ellipsoids with semiaxes (radii) of length a and $b = c$. The shape of these ellipsoids can be estimated for hydrated (bonding

(40) Jelinski et al. have recently demonstrated that NOE experiments employing gated-decoupling techniques may result in an underestimate of the NOE unless the delay time, t_d, is sufficiently long relative to the proton relaxation time (*J. Magn. Reson.*, **41**, 133, (1980)). They observed that a minimum value of ~1.8 for the ratio of t_d to the proton T_1 was needed in order to arrive at accurate NOE values. This is close to the ratio of ~1.6 used in our experiments. We estimate that no more than 20% error in the reported NOE measurements of Table IV would result from this effect.

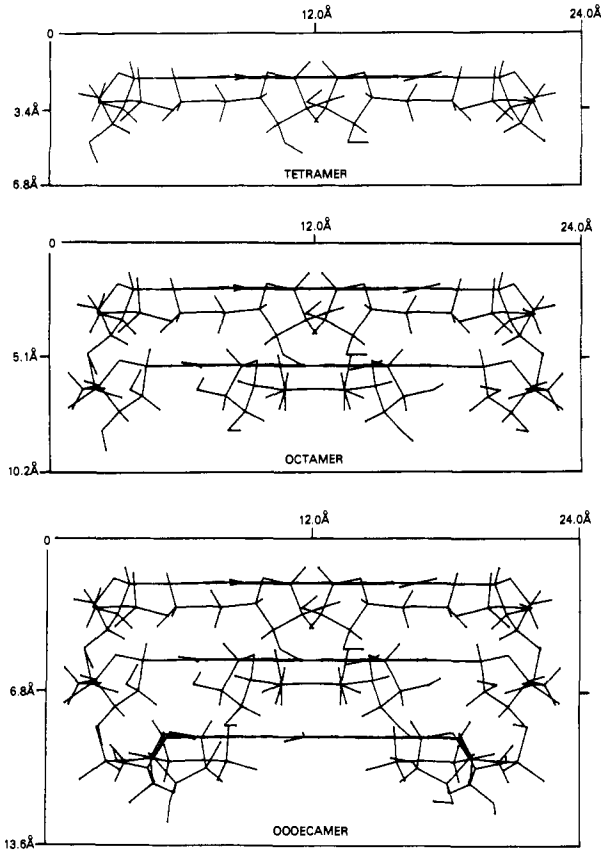

Figure 8. Models for self-associated 5′-GMP stacked in a head-to-tail sense with 30° twist. The structures were computer generated to determine radii *a* (tetramer = 3.4 Å, octamer = 5.1 Å, dodecamer = 5.8 Å) and *b* (= 12 Å) for molecular dynamics calculations discussed in the text. These dimensions allow for van der Waals radii of 1.5, 1.78 and 1.2 Å for oxygen, carbon, and hydrogen atoms, respectively.[41]

of solvent D_2O to polar groups) or unhydrated molecular dimensions and expressed in terms of the ratio $\rho = b/a$. In the case of a sphere $\rho = 1$, while $\rho > 1$ for disk-shaped and $\rho < 1$ for rod-shaped particles. Using a computer molecular display of the HT 30° structure (Figure 8) and standard values for atomic van der Waals radii,[41] we estimate dimensions *a* and *b* of the unhydrated 5′-GMP planar tetramer to be 3.4 and 12 Å, respectively ($\rho = 3.53$). Addition of a molecule of water to each dimension[42] leads to values of 6.4 and 15 Å, while consideration of Na^+ coordination to the phosphate may justify increasing the value of *b* to 16 Å ($\rho = 2.50$) for the maximum estimate of the dimensions of the tetramer. Progressive stacking of one tetramer on another would result in incremental increases of about 1.7 Å in dimension *a* and the concomitant change in ρ from that of an oblate ellipsoid to that of a prolate ellipsoid.

Woessner[24] has shown, by using the rotational diffusion theory of Perrin,[43] that the spectral densities upon which Solomon's[20] dipole relaxation theory depends may be calculated directly from molecular dimensions and a knowledge of the solution viscosity. We have used Woessner's treatment along with programs devised by Torchia et al.[36] (details are given in the supplementary material) to calculate T_1, T_2, and NOE values for 5′-GMP complexes as stacking progresses from a tetramer to a 60-mer, using a temperature of 278 K and a solutioin viscosity η of 0.0742 P (0.70 M 5′-GMP in D_2O, 5 °C). Initially, we determined the NMR

(41) A. Bondi, *J. Phys. Chem.*, **68**, 441 (1964).
(42) J. T. Edward, *J. Chem. Educ.*, **47**, 261 (1970).
(43) F. Perrin, *J. Phys. Radium*, **5**, 497 (1936).

Table IV. Comparison of Experimental and Calculated ^{13}C Relaxation Parameters for 5′-GMP

	T_1,[a] s	$\Delta\nu_{1/2}$,[b] Hz	NOE[c]
	Experimental		
C8a	0.53	37	1.2
C8b	0.32	31	1.4
C8c	0.38	54	1.3
C8d	0.54	40	1.2
	Calculated[d]		
hydrated octamer *a* = 8.1 Å *b* = 16 Å	0.55	29	1.15
unhydrated 40-mer *a* = 18.7 Å *b* = 12 Å	0.57	30	1.15

[a] Conditions as in Figure 7. [b] From Table III. [c] Experimental conditions:[40] 0.74 M in D_2O, 7 °C, 14K acquisitions, 40-μs 90° pulse, 0.27-s acquisition time, 4-s pulse delay. Note the NOE reported here is a ratio of intensities $(1 + \eta)$.[18] [d] Calculated as described in the text from values for σ and τ_R listed in Table V of the supplementary material.

relaxation parameters for a sphere of a volume equivalent to each *n*-mer ellipsoid. We then evaluated the extent of anisotropic rotation in each *n*-mer, permitting calculation of values of rotational correlation times, T_1, T_2, and NOE values.

The experimentally determined relaxation times for the C8 species I (C8a and C8d) are $T_1 = 0.54$ s, $\Delta\nu_{1/2} = 38$ Hz, and NOE = 1.2 (Table IV). From the calculations, two *n*-mers resulted in a good match with these data: a hydrated octomer and an unhydrated 40-mer (Table IV). These two possibilities result from the fact that we do not know with certainty the exact dimensions to select for a 5′-GMP tetramer. Choice of slightly different values from those of Table IV, or variation in the microviscosity from that measured, would generate even more candidates. We do feel, however, the calculation is instructive in defining limits in the range of possibilities and note the close match of experimental data to the "hydrated octamer" species tumbling in a medium of the viscosity of 0.7 M $Na_2$5′-GMP. This coincides with evidence cited earlier on the size of the self-assembled 5′-GMP *n*-mer. The experimental T_1 values for the remaining C8 lines (C8b and C8c) are of the same order of magnitude as the C8a and C8d lines discussed above (Table IV). This suggests they are due to species of comparable size and may be HH and TT structures.

Conclusion

The most stable species formed in the self-structuring of $Na_2$5′-GMP is a head-to-tail octamer, formed by the association of two tetrameric plates. The rotational correlation time of the octamer C8–H8 bond is slow on the NMR time scale, resulting in T_1 values in excess of 0.5 s. At least three other structured species are present in solution with the octamer, probably representing stacked complexes of lower stability.

Acknowledgment. We express our gratitude to David Raiford for expert technical assistance, to Che-Hung Lee for help with the ring-current calculations, and to Dennis Torchia for many helpful discussions during the course of this work. We also acknowledge the contributions of Steven L. Patt, formerly of Stanford Magnetic Resonance Laboratory, who obtained all the 360-MHz spectra for this study.

Registry No. $Na_2$5′-GMP, 5550-12-9.

Supplementary Material Available: Calculation of T_1, T_2, and NOE values for stacked 5′-GMP, table for calculated rotational diffusion parameters for 5′-GMP *n*-mers, and figure showing calculated T_1 values as a function of τ_R (6 pages). Ordering information is given on any current masthead page.